Anomalous Hall effect and current spin polarization in Co_2FeX (X = Al, Ga, In, Si, Ge, and Sn) Heusler compounds: A systematic *ab initio* study

Hung-Lung Huang,[1] Jen-Chuan Tung,[1, 2, 3, *] and Guang-Yu Guo[1, 2, †]

[1]*Department of Physics, National Taiwan University, Taipei 10617, Taiwan*
[2]*Graduate Institute of Applied Physics, National Chengchi University, Taipei 11605, Taiwan*
[3]*Center for General Education, China Medical University, Taichung 40402, Taiwan*
(Dated: July 26, 2021)

Co-based Heusler compounds are ferromagnetic with a high Curie temperature and a large magnetization density, and thus are promising for spintronic applications. In this paper, we perform a systematic *ab initio* study of two principal spin-related phenomena, namely, anomalous Hall effect and current spin polarization, in Co_2Fe-based Heusler compounds Co_2FeX (X = Al, Ga, In, Si, Ge, Sn) in the cubic $L2_1$ structure within the density functional theory with the generalized gradient approximation (GGA). The accurate all-electron full-potential linearized augmented plane-wave method is used. First, we find that the spin-polarization of the longitudinal current (P^L) in Co_2FeX (X = Al, Ga, In, $Al_{0.5}Si_{0.5}$ and Sn) is ∼100 % even though that of the electronic states at the Fermi level (P^D) is not. Further, the other compounds also have a high current spin polarization with $P^L > 85$ %. This indicates that all the Co_2FeX compounds considered are promising for spin-transport devices. Interestingly, P^D is negative in Co_2FeX (X = Si, Ge and Sn), differing in sign from the P^L as well as that from the transport experiments. Second, the calculated anomalous Hall conductivities (AHCs) are moderate, being within 200 S/cm, and agree well with the available experiments on highly $L2_1$ ordered Co_2FeSi specimen although they differ significantly from the reported experiments on other compounds where the B2 antisite disorders were present. Surprisingly, the AHC in Co_2FeSi decreases and then changes sign when Si is replaced by Ge and finally by Sn. Third, the calculated total magnetic moments agree well with the corresponding experimental ones in all the studied compounds except Co_2FeSi where a difference of 0.3 μ_B/f.u. exists. We also perform the GGA plus on-site Coulomb interaction U calculations in the GGA+U scheme. We find that including the U affects the calculated total magnetic moment, spin polarization and AHC significantly, and in most cases, unfortunately, results in a disagreement with the available experimental results. All these interesting findings are discussed in terms of the underlying band structures.

PACS numbers: 71.20.Be, 72.25.Ba, 75.47.Np, 75.70.Tj

I. INTRODUCTION

Most Co-based Heusler compounds in the cubic $L2_1$ structure are ferromagnetic with a high Curie temperature and a large saturation magnetization.[1] Furthermore, many of them were predicted to be half-metallic[2–5] and hence are of particular interest for spintronics. Therefore, the electronic band structure and magnetic properties of the Co-based Heusler compounds have been intensively investigated both theoretically and experimentally in recent years[1–5]. For example, the total magnetic moments of these materials were found to follow the Slater-Pauling type behavior and the mechanism was explained in terms of the calculated electronic structures[2]. The Curie temperatures of Co-based Heulser compounds were also determined from *ab initio* theoretical calculations and the trends were related to the electronic structures[3].

Half-metallic ferromagnets are characterized by the co-existence of metallic behavior for one spin channel and insulating behavior for the other, and their electronic density of states at the Fermi level is completely spin polarized. Thus, they could in principle offer a fully spin-polarized current and are useful for spin electronic devices. The possible half-metallicity of the Co-based Heusler compounds has been intensively investigated experimentally[6–15] and theoretically[2–5,7,10]. In particular, many point-contact Andreev reflection (PCAR) experiments[6–10] have been carried out on Co_2FeSi and its current spin polarization (P^L) was found to vary from 45 % to 60 %, depending on the substrate and the quality of the contact. A higher P^L of ∼80 % was reported in a nonlocal spin valve (NLSV) experiment[11] on Co_2FeSi. The spin Hall effect experiment[8] showed that the P^L of Co_2FeSi is positive. However, the measured positive current spin polarization is at odds with the predictions of the negative spin polarization of the electronic states at the Fermi level (static spin polarization) (P^D) from the *ab initio* calculations[7,16] with the local density approximation (LDA) or generalized gradient approximation (GGA)[17]. Furthermore, the calculated spin magnetic moment (m_s^{tot}) was found to differ by nearly 10 % from the measured total magnetic moment (m^{tot}) of ∼6 μ_B/f.u.[16] It was argued that the Co-based Heusler compounds are strongly correlated systems and hence should be better described by, e.g., the LDA/GGA plus onsite Coulomb Repulsion (U) (LDA/GGA+U) approach[18]. The GGA+U calculations[16] indeed would give rise to a m_s^{tot} of 6 μ_B/f.u. and a positive P^D of 100 % (i.e., being half-metallic). However, the calculated P^D is much larger than the measured spin polarization. Nevertheless,

as pointed out recently in Ref. 7, the spin polarization measured in transport experiments such as PCAR and NLSV experiments should be compared with the theoretical current spin polarization (P^L) rather than static spin polarization (P^D). Therefore, one of the principal purposes of this work is to understand the measured spin polarization in all the Co$_2$FeX compounds by performing a systematic *ab initio* GGA study of both the current and static spin polarizations as well as the total magnetic moment in these compounds. Indeed, we find that the calculated P^L values for the Co$_2$FeX compounds agree with the available experimental results not only in sign but also in magnitude, while the calculated P^D values for Co$_2$FeX (X = Si, Ge and Sn) are wrong even in sign.

The anomalous Hall effect (AHE), discovered in 1881 by Hall[19], is an archetypal spin-related transport phenomenon and hence has recently received renewed attention[20]. Indeed, many *ab initio* studies on the AHE in elemental ferromagnets[21–24] and intermetallic alloys[25,26] have recently been reported. However, *ab initio* investigations into the AHE in the Heusler compounds have been few[5,27,28]. Interestingly, Co$_2$MnX (X = Al, Ga and In) were recently predicted[5] to have a large intrinsic anomalous Hall conductivity (AHC) in the order of ~1000 S/cm, and thus could find applications in magnetization sensors[29]. Therefore, another principal purpose of this work is to understand the AHE in all the Co$_2$Fe-based Heusler compounds and the results may help experimental search for the Heusler compounds with large AHE for applications. Furthermore, by comparison of the calculated AHC as well as the current spin polarization and total magnetic moment with the measured ones, one could have a comprehensive assessment of whether or not the Co$_2$FeX compounds are strongly correlated systems that would require the GGA+U approach.

In nonmagnetic materials where the numbers of the spin-up and spin-down electrons are equal, the opposite transverse currents caused by the applied electric field would result in a pure spin current, and this is known as the intrinsic spin Hall effect (SHE).[30] The pure spin current is dissipationless[30] and is thus important for the development of low energy-consumption nanoscale spintronic devices[31]. We note that high spin-polarization (P^L) of the charge current (I_C) from the electrode is essential for large giant magnetoresistance (GMR)[32,33] and tunneling magnetoresistance (TMR)[34,35]. However, since the current-induced magnetization switching results from the transfer of spin angular momentum from the current carriers to the magnet[36], large spin current (I_S) would be needed for the operation of the spin-torque switching-based nanodevices[36,37], i.e., a large ratio of spin current to charge current [$\eta = |(2e/\hbar)I_S/I_C|$], would be crucial. For ordinary charge currents, this ratio η varies from 0.0 (spin unpolarized current) to 1.0 (fully spin polarized current). Interestingly, η can be larger than 1.0 for the Hall currents and is ∞ for pure spin current. Fascinatingly, spin-torque switching of ferromagnets driven by pure spin current from large SHE in tantalum has been

recently reported[31]. Therefore, it might be advantageous to use the Hall current from ferromagnets for magneto-electronic devices, rather than the longitudinal current. Another purpose of this work is therefore to investigate the nature and spin-polarization of the Hall current in the Co$_2$Fe-based Heusler compounds for possible spintronic applications.

The rest of this paper is organized as follows. In the next section, we briefly describe the theories of the intrinsic anomalous and spin Hall conductivities as well as Hall and longitudinal current spin polarizations. We will also introduce the full-potential relativistic band theoretical method used and give the computional details. In Sec. III, the calculated magnetic moments, intrinsic Hall conductivities and current spin polarizations of all the studied Co$_2$FeX compounds will be reported in subsections III (A), (B) and (C), respectively. The theoretical results will be analyzed in terms of the underlying band structures and also compared with the available experimental ones. In subsection III (D), the results from the GGA+U calculations will be presented to examine the effect of including the semi-empirical on-site Coulomb interaction on the calculated physical properties of the Co$_2$FeX compounds. Finally, conclusions drawn from this work will be given in Sec. IV.

II. THEORY AND COMPUTATIONAL METHOD

We first perform the self-consistent electronic structure calculations for the Co$_2$FeX compounds within the density functional theory with the GGA for the exchange correlation potential[17]. Since all the intrinsic Hall effects are caused by the relativistic electron spin-orbit interaction, the spin-orbit coupling (SOC) is included in the present *ab initio* calculations. We use the highly accurate full-potential linearized augmented plane wave (FLAPW) method, as implemented in the WIEN2K code[38]. The wave function, charge density, and potential were expanded in terms of the spherical harmonics inside the muffin-tin spheres and the cutoff angular moment (L_{max}) used is 10, 6 and 6, respectively. The wave function outside the muffin-tin spheres is expanded in terms of the augmented plane waves (APWs) and a large number of APWs (about 70 APWs per atom, i. e., the maximum size of the crystal momentum $K_{max} = 8/R_{mt}$) were included in the present calculations. The improved tetrahedron method is used for the Brillouin-zone integration[39]. To obtain accurate ground state charge density as well as spin and orbital magnetic moments, a fine $27\times27\times27$ grid with 1470 k-points in the irreducible Brillouin zone wedge (IBZW) is used. The self-consistent cycles were terminated when the integrated charge density variation became less than 10^{-5} e.

We consider the Co$_2$FeX Heusler compounds in the fully ordered cubic L2$_1$ structure. The available experimental lattice constants[40] are used for all the consid-

ered Co$_2$FeX (X = Al, Ga, In, Si, Ge, Sn) Heusler alloys except Co$_2$FeAl$_{0.5}$Si$_{0.5}$, Co$_2$FeIn and Co$_2$FeSn, as listed in Table I. Since the experimental lattice constant for Co$_2$FeIn is not available, we determine the lattice constant for Co$_2$FeIn theoretically, also by using the FLAPW method, as described in the preceding paragraph. We also study the L2$_1$ Co$_2$FeAl$_{0.5}$Si$_{0.5}$ alloy and model it by the virtual crystal approximation (VCA), i.e., the Al/Si site is occupied by a virtual atom with the atom number $Z = 0.5Z_{Al} + 0.5Z_{Si}$, where Z_{Al} and Z_{Si} are the Al and Si atomic numbers, respectively. The lattice constant of 5.689 Å, which is the average of the experimental lattice constants of Co$_2$FeAl (5.737 Å) and Co$_2$FeSi (5.640 Å), is used for Co$_2$FeAl$_{0.5}$Si$_{0.5}$ because the lattice constant of the Co$_2$FeAl$_x$Si$_{1-x}$ alloy was reported to depend linearly on the Al concentration (x)[45]. Note that in fact we have determined the lattice constants theoretically also for the Co$_2$FeX (X = Al, Ga, Si, Ge) compounds. The theoretical lattice constants for these compounds differ from the experimental values by less than 1 %. As a result, the physical properties of these compounds calculated using the experimental and theoretical lattice constants differ only slightly. Therefore, for simplicity, we present only the physical properties of these compounds calculated using the experimental lattice constants in the next section. However, the theoretical lattice constant (6.013 Å) of Co$_2$FeSn is 2.4 % larger than the experimental one (5.87 Å)[46] perhaps because the prepared Co$_2$FeSn films contained only a low degree of L2$_1$ order. Therefore, the theoretical lattice constant is used for Co$_2$FeSn (Table I).

A. Anomalous and spin Hall conductivities

The intrinsic anomalous and spin Hall conductivities of a solid can be evaluated by using the Kubo formalism.[21,47,48] Here we first calculate the imaginary part of the off-diagonal elements of the optical conductivity. Then we obtain the real part of the off-diagonal elements from the imaginary part by a Kramers-Kronig transformation. The intrinsic AHC (σ_{xy}^A) is the static limit of the off-diagonal element of the optical conductivity $\sigma_{xy}^{(1)}(\omega = 0)$. If we now replace the charge current operator $-e\hat{\mathbf{v}}$ with the spin current operator $(\hbar/4)\{\Sigma_z, \hat{\mathbf{v}}\}$ and repeat the calculation[47], we will obtain the intrinsic spin Hall conductivity (SHC) (σ_{xy}^S). We note in passing that alternatively, one could also calculate σ_{xy}^A (σ_{xy}^S) by an integration of the (spin) Berry curvature over the Brillouin zone[21,49,50]. Nevertheless, the two methods were found to be numerically equivalent[21,49,50].

A dense k point mesh would be needed for obtaining accurate AHC and SHC[21,48]. Therefore, we use several fine k-point meshes with the finest k-point mesh being $58 \times 58 \times 58$ which has 8125 k-points in the IBZW. We calculate the AHC and SHC as a function of the number (N_k) of k-points in the first Brillouin zone. The calculated AHC (σ_{xy}^A) and SHC (σ_{xy}^S) versus the inverse of the N_k are then plotted and fitted to a polynomial to get the

converged theoretical σ_{xy}^A and σ_{xy}^S (i.e., the extrapolated value at $N_k = \infty$) (see Refs. 23 and 24). Furthermore, to ensure that the $\sigma_{xy}^{(1)}(\omega = 0)$ via the Kramers-Kronig transformation is accurate, the energy bands up to 5.5 Ry are included in the calculation of $\sigma_{xy}^{(2)}(\omega)$.

B. Current spin polarization

The spin polarization of a magnetic material is usually described in terms of the spin-decomposed densities of states (DOSs) at the Fermi level (E_F) as follows

$$P^D = \frac{N_\uparrow(E_F) - N_\downarrow(E_F)}{N_\uparrow(E_F) + N_\downarrow(E_F)}, \tag{1}$$

where $N_\uparrow(E_F)$ and $N_\downarrow(E_F)$ are the spin-up and spin-down DOSs at the E_F, respectively. This static spin polarization P^D would then vary from -1.0 to 1.0 only. For the half-metallic materials, P^D equals to either -1.0 or 1.0. As mentioned above, the spin polarization P^D defined by Eq. (1) is not necessarily the spin polarization of the transport currents measured in experiments. Indeed, the spin-polarizations measured by using different experimental techniques could differ significantly[51–54]. From the viewpoint of spintronic applications, only the current spin polarization instead of the P^D, counts.

Therefore, in this work, we further calculate the spin polarization of both the longitudinal and Hall currents, as described below. Here, we calculate the longitudinal electric conductivities ($\sigma_\uparrow, \sigma_\downarrow$) for spin-up and spin-down electrons divided by the corresponding Drude relaxation times ($\tau_\uparrow, \tau_\downarrow$) (i.e., $\sigma_\uparrow/\tau_\uparrow, \sigma_\downarrow/\tau_\downarrow$) within the semi-classical Boltzmann transport theory, as implemented in Boltz-Trap code[55]. In the present calculations, the relaxation time is assumed to be independent of energy, k-point and spin direction (i.e., $\tau_\uparrow = \tau_\downarrow = \tau$). Consequently, we can obtain the longitudinal current spin polarization P^L from

$$P^L = \frac{\sigma^\uparrow - \sigma^\downarrow}{\sigma^\uparrow + \sigma^\downarrow} \simeq \frac{\sigma^\uparrow/\tau - \sigma^\downarrow/\tau}{\sigma^\uparrow/\tau + \sigma^\downarrow/\tau}. \tag{2}$$

The underlying scalar-relativistic band structures are calculated by using a fine $36 \times 36 \times 36$ mesh with 3349 k-points in the IBZW.

The spin polarization P^H of the Hall current may be written as[5,24]

$$P^H = \frac{\sigma_{xy}^{H\uparrow} - \sigma_{xy}^{H\downarrow}}{\sigma_{xy}^{H\uparrow} + \sigma_{xy}^{H\downarrow}} \tag{3}$$

where $\sigma_{xy}^{H\uparrow}$ and $\sigma_{xy}^{H\downarrow}$ are the spin-up and spin-down Hall conductivities, respectively. The $\sigma_{xy}^{H\uparrow}$ and $\sigma_{xy}^{H\downarrow}$ can be obtained from the calculated AHC and SHC via the relations[50]

$$\sigma_{xy}^A = \sigma_{xy}^{H\uparrow} + \sigma_{xy}^{H\downarrow} \tag{4}$$

$$-2\frac{e}{\hbar}\sigma_{xy}^S = \sigma_{xy}^{H\uparrow} - \sigma_{xy}^{H\downarrow}. \tag{5}$$

Note that, the absolute value of P^H can be greater than 1.0 because the spin-decomposed Hall currents can go either right (positive) or left (negative). In the non-magnetic materials, the charge Hall current is zero, and hence, $\sigma_{xy}^{H\uparrow} = -\sigma_{xy}^{H\downarrow}$ results in $P^H = \infty$. Clearly, in the case of Hall currents, the ratio of the spin current to charge current $\eta = |(2e/\hbar)\sigma_{xy}^S/\sigma_{xy}^A| = |P^H|$.

III. RESULTS AND DISCUSSION

A. Magnetic moments and band structure

Let us first examine the calculated magnetic properties and band structures near the Fermi level of the considered Co_2FeX Heusler alloys. Since the electronic structure and magnetism in the full Heusler compounds have been extensively studied (see, e.g., Refs. 2–4 and references therein), here we focus on only the salient features which may be related to the anomalous and spin Hall effects as well as current spin polarizations to be presented in the next subsections. The calculated total magnetic moment, total spin magnetic moment, local spin and orbital magnetic moments as well as spin-decomposed DOSs at E_F of all the considered Co_2FeX Heusler alloys are listed in Table I, together with the available experimental total magnetic moments for comparison. The total and site decomposed DOSs of three selected Heusler compounds Co_2FeAl, $Co_2FeAl_{0.5}Si_{0.5}$ and Co_2FeSi are displayed in Fig. 1. The scalar relativistic band structures of Co_2FeAl and Co_2FeSi are shown in Figs. 2(a) and 2(c), respectively.

Interestingly, the studied Heusler alloys could be separated into two groups according to the calculated DOS at E_F. In one group, including Co_2FeAl, Co_2FeGa, $Co_2FeAl_{0.5}Si_{0.5}$ and Co_2FeIn, the majority spin state dominates. In the other group, including Co_2FeSi, Co_2FeGe and Co_2FeSn, the minority spin state dominates (see Table I). Therefore, the calculated spin polarization (P^D) for the first group is positive while that of the second group is negative (see Table II). It is clear from Fig. 1(a) that there is a band gap near the E_F for the minority spin channel in Co_2FeAl and adding one valance electron can be approximatively treated as raising the E_F by ~ 0.4 eV. This E_F shift is nearly equal to that from Co_2MnAl to Co_2MnSi in Ref. 5 where the calculated P^D for both compounds, however, is positive. This is because the minority gap here is small, being ~ 0.2 eV, while that in Co_2MnAl is much larger, being ~ 0.8 eV.

Figure 1 and Table I show that from the view point of the calculated band structures, all the considered Heusler compounds are not half-metallic, although Co_2FeAl is nearly a half-metal because its E_F just touches the bottom of the minority spin conduction band [Fig. 2(a)]. Previous GGA calculations[58] also predicted that of Co_2FeAl, $Co_2FeAl_{0.5}Si_{0.5}$ and Co_2FeSi are not half-metallic. The DOS spectra for Co_2FeAl, $Co_2FeAl_{0.5}Si_{0.5}$,
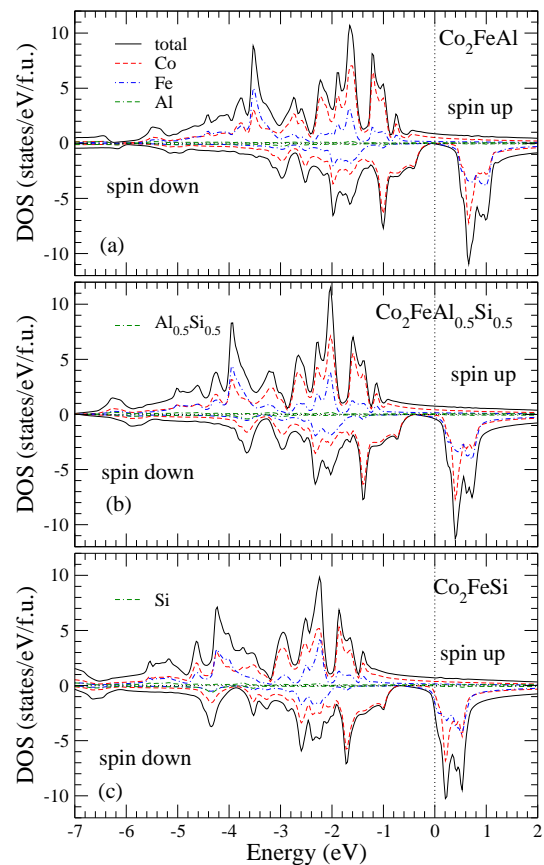

FIG. 1. (color online) Total and site decomposed density of states (DOS) for (a) Co_2FeAl, (b) $Co_2FeAl_0.5Si_0.5$ and (c) Co_2FeSi. The Fermi level is at zero.

and Co_2FeSi are similar and differ only in the location of E_F (see Fig. 1). The DOS spectra of Co_2FeGa (Co_2FeIn) and Co_2FeGe (Co_2FeSn) (not shown here) also look similar, except the location of E_F.

Table I indicates that among the considered Heusler compounds, only the total spin magnetic moment m_s^{tot} of Co_2FeAl and Co_2FeGa almost satisfies the so-called generalized Slater-Pauling rule $m_s^{tot} = n_v - 24$ where n_v is the number of valence electrons[2]. This may be expected because none of these compounds is predicted to be half-metallic here and only Co_2FeAl is nearly half-metallic. Table I also suggests that the calculated m^{tot} agrees well with the available measured one for all the considered compounds except Co_2FeSi. The discrepancy between the calculated and experimental m^{tot} is ~ 0.3 μ_B/f.u. for Co_2FeSi but is about 0.1 μ_B/f.u. or less for all the other compounds (Table I).

B. Anomalous and spin Hall conductivities

The calculated anomalous Hall conductivity σ_{xy}^A and spin Hall conductivity σ_{xy}^S for all the studied compounds are listed in Table II. We notice that compared with the

TABLE I. Calculated total spin magnetic moment (m_s^{tot}) $(\mu_B/\text{f.u.})$, atomic spin (m_s) and orbital (m_o) magnetic moments (μ_B/atom) as well as spin-decomposed density of states at the Fermi level $[N^\uparrow(E_F), N^\downarrow(E_F)]$ (states/eV/f.u.) of all the considered Co_2FeX Heusler compounds together with the lattice constants a (Å) used. The available experimental magnetic moments[41–44] (Exp.) are also listed for comparison with the calculated total magnetic moments (m^{tot}) $(\mu_B/\text{f.u.})$. In $Co_2FeAl_{0.5}Si_{0.5}$, listed in the bracket is the spin magnetic moment of Si. The orbital magnetic moments for the non-transition metal atoms (m_o^X) are less than 0.0001 μ_B/atom and hence not listed here. The theoretical total magnetic moment (m^{tot}) is given by $m^{tot} = m_s^{tot} + 2m_o^{Co} + m_o^{Fe}$, which should be compared with the experimental magnetic moment.

Co_2FeX	a		m^{tot}	m_s^{tot}	m_s^{Co}	m_s^{Fe}	m_s^X	m_o^{Co}	m_o^{Fe}	$N^\uparrow(E_F)$	$N^\downarrow(E_F)$
Co_2FeAl	5.737^a	GGA	5.123	4.993	1.229	2.788	-0.064	0.041	0.048	0.862	0.059
		Exp.	4.96								
Co_2FeGa	5.751^a	GGA	5.149	5.016	1.206	2.811	-0.047	0.041	0.051	0.885	0.189
		Exp.	5.13								
Co_2FeIn	5.990	GGA	5.308	5.143	1.250	2.885	-0.046	0.052	0.061	0.859	0.575
$Co_2FeAl_{0.5}Si_{0.5}$	5.689	GGA	5.523	5.376	1.338	2.683	-0.037	0.052	0.043	0.755	0.399
Co_2FeSi	5.640^a	GGA	5.688	5.541	1.388	2.848	-0.002	0.040	0.067	0.714	2.476
		Exp.	5.97								
Co_2FeGe	5.743^a	GGA	5.854	5.693	1.422	2.917	0.012	0.046	0.069	0.785	2.288
		Exp.	5.90, 5.74								
Co_2FeSn	6.013	GGA	5.994	5.797	1.445	3.021	-0.005	0.060	0.079	0.712	2.457

^{a} Experimental lattice constants[40].

TABLE II. Calculated anomalous $[\sigma_{xy}^A$ (S/cm)$]$ and spin $[\sigma_{xy}^S$ ($\hbar$S/e cm)$]$ Hall conductivities, spin-decomposed Hall conductivities $(\sigma_{xy}^{H\uparrow}, \sigma_{xy}^{H\downarrow})$ (S/cm), Hall (P^H) and longitudinal (P^L) current spin polarizations (%) as well as spin polarization of the electronic states at the Fermi level P^D (%) of all the considered Heusler compounds Co_2FeX. The available experimental spin polarization and scattering-independent part $(b)^{56}$ of the σ_{xy}^A are also listed for comparison. Note that b contains both the intrinsic contribution (σ_{xy}^A) calculated here and also the extrinsic side-jump contribution (σ_{xy}^{A-sj}).

Co_2FeX		σ_{xy}^A, b	σ_{xy}^S	$\sigma_{xy}^{H\uparrow}$	$\sigma_{xy}^{H\downarrow}$	P^H	P^L	P^D
Co_2FeAl	GGA	39	35	-16	55	-180	100	87
	Exp.	$320\sim360^a$					56^b	
Co_2FeGa	GGA	181	56	35	147	-62	98	65
	Exp.						57^c	
Co_2FeIn	GGA	102	56	-5	107	-110	92	20
$Co_2FeAl_{0.5}Si_{0.5}$	GGA	124	74	-12	136	-119	92	31
	Exp.	$-100\sim50^g, 352^h$					60^e	
Co_2FeSi	GGA	189	24	71	119	-25	86	-55
	Exp.	$163^d, 300\sim600^a$					$45\sim60^e, 80^f$	
Co_2FeGe	GGA	119	-29	89	31	49	89	-49
	Exp.						59^c	
Co_2FeSn	GGA	-78	-24	-15	-63	-62	93	-55

^{a} Experimental b values from sputtered films with the B2 structure[13].
^{b} Point-contact Andreev reflection experiments[12].
^{c} Point-contact Andreev reflection experiments on $Co_2FeGa_xGe_{1-x}$ in the L2$_1$/B2 mixed structure[15].
^{d} Experimental b value from Co_2FeSi single crystals with the L2$_1$ structure[6].
^{e} Point-contact Andreev reflection experiments[7,9,10,45].
^{f} Nonlocal spin-valve experiment[11].
^{g} Experimental b values from sputtered $Co_2FeAl_{0.4}Si_{0.6}$ films with the B2 structure[57].
^{h} Experimental b value from sputterd ultrathin $Co_2FeAl_{0.5}Si_{0.5}$ film with the B2 structure[14].

AHC of Fe metal[21] and also Co_2MnX (X = Al, Ga and In)[5], the σ_{xy}^A of the present Heusler compounds is moderate in magnitude, being within 200 S/cm (Table II). In fact, the AHC of Co_2FeX (X = Al, Ga and In) (Table II) is about one order of magnitude smaller than the corresponding Co_2MnX (X = Al, Ga and In) (see Table II in Ref. 5). This can be explained in terms of the calculated band structure and also σ_{xy}^A as a function of E_F in Co_2FeAl (Figs. 2a and 2b). Figures 2a and 2c show that the spin-up bands near E_F are the highly dispersive Co *spd*, Fe *spd* and Al *sp* hybridized bands while E_F nearly falls within the spin-down band gap. Conse-

quently, the σ_{xy}^A is rather small (being $\sim$35 S/cm) (see Fig. 2b). However, when E_F is lowered to below -0.8 eV, σ_{xy}^A increases dramatically to the values of $\sim$1000 S/cm (Fig. 2b). These large σ_{xy}^A values come mainly from the spin-up Co d dominant bands in this energy range (Figs. 2a and 2c). In Co_2MnAl, the corresponding spin-up Co d dominant bands are higher in energy, and the E_F is lower because Co_2MnAl has one fewer valence electron than Co_2FeAl. As a result, the E_F sits on the Co d dominant σ_{xy}^A peak in Co_2MnAl and thus Co_2MnAl has a much larger σ_{xy}^A (being $\sim$ 1300 S/cm).[5] This interesting finding suggests a way to chemical composition tuning of the AHC in $Co_2Mn_{1-x}Fe_xX$ (X = Al, Ga and In) alloys.

Interestingly, for the Co_2FeX (X = Si, Ge and Sn) compounds, the AHC gets reduced when Si is replaced by Ge and changes sign when Ge is further substituted by Sn. Nevertheless, the calculated band structures for the Co_2FeX (X = Si, Ge and Sn) compounds look very similar, especilly in the vinicity of E_F. Thus, there is no obvious explanation for this interesting evolution. Table II indicates that the σ_{xy}^A of Co_2FeSi is about five times larger than that of Co_2FeAl. This could be attributed to the band filling effect. Figure 2 shows that in Co_2FeSi, due to the additional one valence electron, the E_F is raised to the bottom of the $Co/Fe\ d(e_g)$ dominant bands where σ_{xy}^A is large (Fig. 2b), thus resulting in a much larger σ_{xy}^A.

Several AHE experiments on the Co_2FeX compounds and their alloys have been carried out.[6,13,14,57] The derived AHC values (b)[56] for Co_2FeAl, $Co_2FeAl_{0.5}Si_{0.5}$ and Co_2FeSi are listed in Table II. However, quantitative comparison of the present theoretical calculations with the experimental results is difficult, because all the samples used in the experiments except Co_2FeSi are in the B2 structure with antisite disorders (Table II). The deduced AHC values depend strongly on the substrates used and annealing temperatures which control the degree of the B2 antisite disorders and also the defect concentrations.[13,57] Nevertheless, Table II shows that the calculated σ_{xy}^A of Co_2FeSi is in good agreement with the experimental result from the single crystal sample[6], indicating the intrinsic AHC σ_{xy}^A dominates in Co_2FeSi single crystals with the L2_1 structure. In contrast, the theoretical σ_{xy}^A of Co_2FeAl is one order of magnitude smaller than the b derived from the experiment[13]. For $Co_2FeAl_{0.5}Si_{0.5}$, the b values from two different experiments[14,57] are very different, suggesting the important influences of the B2 antisite disorder and also the substrate. We could attribute the pronounced discrepancies between the theoretical (intrinsic) (σ_{xy}^A) and experimental b values[13] of Co_2FeAl and Co_2FeSi to a significant contribution from the impurity side-jump scattering as well as the structural difference. However, recent *ab initio* calculations[27] for Co_2CrAl and Co_2MnAl indicated that the B2 antisite disorders tend to significantly reduce the intrinsic AHC σ_{xy}^A. Therefore, in the experiments[13] on Co_2FeAl and Co_2FeSi, side-jump mechanism could dominate and thus

result in a much larger b than σ_{xy}^A.

Table II indicates that the calculated σ_{xy}^S in Co_2FeIn and $Co_2FeAl_{0.5}Si_{0.5}$ is about half of the σ_{xy}^A and their Hall current spin polarization (P^H) is nearly 100 %. In a half-metal, the charge current would flow only in one spin channel and no charge current in the other spin channel, thus resulting in σ_{xy}^A being twice as large as σ_{xy}^S. Therefore, Co_2FeIn and $Co_2FeAl_{0.5}Si_{0.5}$ may be called anomalous Hall half-metals[5], even though their electronic states near E_F are far from fully spin-polarized (see P^D in Table II). Finally, we note that the ratio of spin current to charge current for the Hall current $(\eta = |P^H|)$ in Co_2FeAl is large with $\eta > 150$ %.

C. Current spin polarizations

The calculated spin polarizations of Hall (P^H) and longitudinal (P^L) currents as well as electronic states at E_F (P^D) for all the Heusler componds considered here are listed in Table II. Also listed in Table II are the spin-decomposed Hall conductivities $(\sigma_{xy}^{H\uparrow}$ and $\sigma_{xy}^{H\downarrow})$ obtained using Eqs. (4) and (5). Remarkably, Table II shows that the calculated P^L is nearly 100 % in Co_2FeAl, Co_2FeGa and $Co_2FeAl_{0.5}Si_{0.5}$ even though their P^D is significantly smaller than 100 %. This finding, therefore, indicates that these Heusler compounds are half-metallic from the viewpoint of charge transport, even though their electronic band structures are not. All the other compounds also have a high current spin polarization with $P^L > 85$ %. Therefore, all the Heusler compounds considered here may find valuable applications in spintronic devices. Interestingly, Table II also demonstrates that the P^L and P^D in Co_2FeSi, Co_2FeGe and Co_2FeSn could even have opposite signs. The calculated current spin polarization P^L in Co_2FeSi and Co_2FeGe is positive, being in good agreement with recent spin Hall effect experiments[8]. In contrast, the static spin polarization (P^D) differs from the experimental spin polarization even in sign (Table II). This clearly urges one to compare the measured spin polarization from transport experiments to the theoretical current spin polarization rather than the static spin polarization which has often been done in the past.

The interesting finding that the P^L and P^D in Co_2FeSi, Co_2FeGe and Co_2FeSn differ in sign, could be explained in terms of the calculated band structures. Figure 2(c) indicates that in Co_2FeSi, for the spin-up channel, the E_F cuts through the highly dispersive Co/Fe spd and Si sp hybridized bands. On the other hand, for the spin-down channel, the E_F is located at the bottom of the Co/Fe $d(e_g)$ dominated bands. Consequently, the spin-down DOS at E_F is higher than the spin-up DOS (see Fig. 1c and Table I), giving rise to the negative value of P^D. From transport viewpoint, however, the spin-down Co/Fe $d(e_g)$ dominated bands which are narrow (Fig. 2c), would have large effective masses and small Fermi velocities, thereby contributing little to the charge current. On the other hand, the spin-up Co/Fe
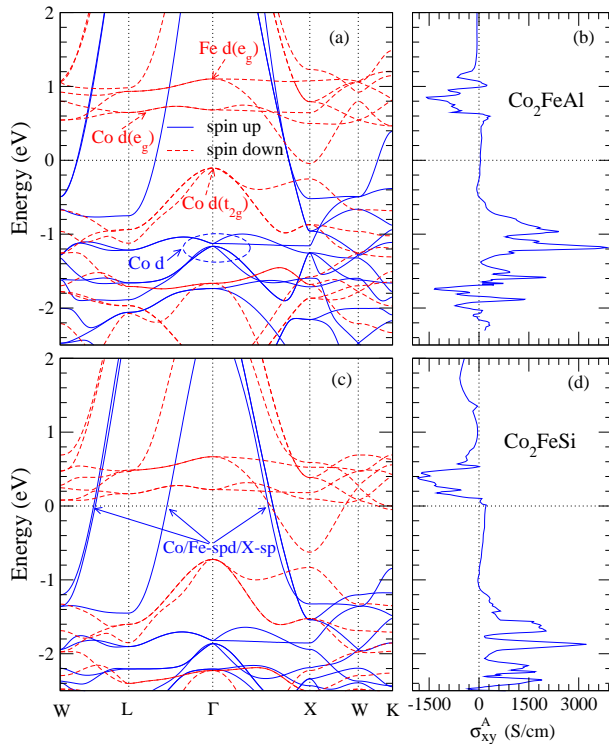
FIG. 2. (color online) Scalar relativistic band structure [(a) and (c)], and anomalous Hall conductivity (σ_{xy}^A) [(b) and (d)] for Co_2FeAl, and Co_2FeSi, respectively. The Fermi energy is at zero.

spd and Si sp hybridized bands which are highly dispersive, would have large Fermi velocities and small effective masses, thus providing the dominant contribution to the charge current. Therefore, the current spin polarization is positive, being in good agreement with the experiments (Table II).

Many experiments[7,9,10,12,15,45] especially PCAR measurements on Co_2Fe-based Heusler alloys have been carried out to determine their spin polarization which is a key factor for their spintronic applications. Majority of these experiments were focused on Co_2FeSi mainly because highly $L2_1$ ordered Co_2FeSi samples could be fabricated. However, the P^L values derived from PCAR experiments on Co_2FeSi vary significantly from 45 % to 60% (Table II), depending on the quality of the samples. This could be expected because the spin polarization determined by a PCAR experiment depends not only on the degree of the ordering and the defects in the sample but also on the quality of the contact and the substrate[59]. Nevertheless, the theoretical P^L value of 86 % agrees rather well with the experimental value of 80% from the nonlocal spin-valve experiment[11] on highly $L2_1$-ordered specimens. However, the measured P^L values for Co_2FeAl, Co_2FeGa and $Co_2FeAl_{0.5}Si_{0.5}$ are around 60 %, which is far from the predicted P^L value of ~100 % for these compounds (Table II). These significant discrepancies may reflect the fact that the samples used in the

experiments[10,12,15] had a high degree of the B2 antisite disorders.

D. Effects of on-site Coulomb interaction

To examine the effect of on-site Coulomb interaction, we further perform the calculations in the GGA+U scheme[18]. The on-site Coulomb repulsion U(exchange interaction J) used are 2.82 (0.9) and 2.6 (0.8) eV for Co and Fe, respectively, which are widely used for Co_2-based Heusler compounds.[58] The results from these GGA+U calculations are compared with those of the GGA calculations in Table III. We notice that the total spin magnetic moments (m_s^{tot}) from the GGA and GGA+U calculations are almost identical in all the Heusler compounds except Co_2FeSi and Co_2FeGe. This may be expected since the GGA m_s^{tot} is already nearly saturated in these compounds. Including the on-site Coulomb interaction increases the m_s^{tot} in Co_2FeSi and Co_2FeGe to the saturation values. Note that the measured magnetic moments should be compared with the calculated total magnetic moments (m^{tot}) instead of total spin magnetic moments (m_s^{tot}) in Tables I and III. The m^{tot} contains both the m_s^{tot} and the total orbital magnetic moment which cannot be neglected in the Heusler compounds studied here because the orbital magnetic moments on the Fe and Co atoms are rather significant (Table I). Tables I and III together show that including the on-site Coulomb interaction actually increases the small discrepancies between the experiments and the GGA calculations found in all the Heusler compounds except Co_2FeSi where the difference of 0.3 μ_B/f.u. is reduced slightly to 0.2 μ_B per formula unit.

Table III shows that the on-site Coulomb interaction has a pronounced effect on the spin polarization. First, the current spin polarization (P^L) for all the studied compounds is now 100 % from the GGA+U calculations. Second, the static spin polarization (P^D) approaches to 100% for all the compounds except Co_2FeGa. Therefore, these Heusler compounds become half-metals in terms of both the band structure and current spin polarization. This may be expected because the main effect of the on-site Coulomb interaction is to raise the spin-down Fe and Co d-dominant conduction bands. Consequently, if sufficiently large U values are used, the spin-down Fe and Co d-dominant conduction bands will move to above E_F. This will open a gap in the spin-down channel and thus give rise to zero spin-down DOS at E_F (Table III). However, the spin-down GGA+U band gap is as large as 0.9 eV in Co_2FeSi, for example, being nearly 100 times larger than the measured one[6]. Interestingly, including Coulomb U changes the spin polarization P^D in Co_2FeSi and Co_2FeGe from negative to positive (Table III). However, it should be emphasized that the mechanism of the spin polarization sign change here is very different from the sign difference between the P^D and P^L in the GGA calculations. Nevertheless, whether the

TABLE III. Total magnetic moment (m^{tot}), total spin magnetic moment (m_s^{tot}) (μ_B/f.u.), spin-decomposed density of states at the Fermi level [$N^\uparrow(E_F)$, $N^\downarrow(E_F)$] (states/eV/f.u.), spin polarization of the electronic states at the Fermi level P^D (%), longitudinal current polarization P^L (%, anomalous [σ_{xy}^A (S/cm)] and spin [σ_{xy}^S ($\hbar$S/e cm)] Hall conductivities and Hall current spin polarization P^H (%) of the Co$_2$FeX Heusler compounds from both the GGA and GGA+U calculations. The on-site Coulomb (exchange) interaction U (J) for Co and Fe used are 2.82 (0.9) eV and 2.6 (0.8) eV, respectively.

Co$_2$FeX		m^{tot}	m_s^{tot}	$N^\uparrow(E_F)$	$N^\downarrow(E_F)$	P^D	P^L	σ_{xy}^A	σ_{xy}^S	P^H
Co$_2$FeAl	GGA	5.123	4.993	0.862	0.059	87	100	39	35	-180
	GGA+U	5.202	4.999	0.753	0.003	99	100	98	69	-140
Co$_2$FeGa	GGA	5.149	5.016	0.885	0.189	65	98	181	56	-62
	GGA+U	5.259	5.043	0.772	0.515	20	100	89	67	-151
Co$_2$FeAl$_{0.5}$Si$_{0.5}$	GGA	5.523	5.376	0.755	0.399	31	92	124	74	-119
	GGA+U	5.700	5.498	0.667	0.001	100	100	139	87	-125
Co$_2$FeSi	GGA	5.688	5.541	0.714	2.476	-55	86	189	24	-25
	GGA+U	6.196	5.998	0.587	0.008	98	100	73	54	-148
Co$_2$FeGe	GGA	5.854	5.693	0.785	2.288	-49	89	119	-29	-49
	GGA+U	6.222	5.997	0.624	0.003	99	100	14	40	-570

P^D is positive or negative can be tested by spin-polarized angle-resolved photoemission experiments which, unfortunately, have not been reported on any Heusler compound studied here.

Table III also indicates that including the on-site Coulomb U changes the calculated AHC and SHC substantially. In particular, the σ_{xy}^A gets reduced significantly for all the studied compounds except Co$_2$FeAl (Table III). For example, the theoretical σ_{xy}^A for Co$_2$FeGe is 119 S/cm from the GGA calculation but is reduced to 14 S/cm when the on-site Coulomb U is included. This suggests that by comparing the calculated σ_{xy}^A with the measured one, one could assess whether or not including on-site Coulomb U is needed to properly describe the electronic properties of a Co$_2$Fe-based Heusler compound. The measured σ_{xy}^A of Co$_2$FeSi[6] is $\sim$160 S/cm, being in good agreement with the GGA result (Table II). However, it is two times larger than the result of the GGA+U calculation (about 70 S/cm). This indicates that Co$_2$Fe-based Heusler compounds are not strongly correlated systems and there may be no need to include the on-site Coulomb U for these compounds.

IV. CONCLUSIONS

We have carried out a systematic *ab initio* study of the anomalous Hall effect and current spin polarization as well as the magnetic properties of the Co$_2$FeX (X = Al, Ga, In, Si, Ge, Sn) Heusler compounds in the cubic L2$_1$ structure by using the highly accurate all-electron FLAPW method. First, we find that the spin-polarization of the longitudinal current (P^L) in Co$_2$FeX

(X = Al, Ga and Al$_{0.5}$Si$_{0.5}$) is $\sim$100 % even though the static spin polarization (P^D) is not. Furthermore, the other compounds also have a high current spin polarization with $P^L > 85$ %. This indicates that all the Co$_2$FeX compounds are promising for spintronic devices. Interestingly, P^D is negative in Co$_2$FeX (X = Si, Ge and Sn), differing in sign from the P^L as well as from that from the transport experiments. Second, the calculated AHCs are moderate, being within 200 S/cm, and agree well with the available experiments on highly L2$_1$ ordered Co$_2$FeSi specimen although they differ significantly from the reported experiments on other compounds where the B2 antisite disorders were present. Surprisingly, the AHC in Co$_2$FeSi decreases and then changes from the negative to positive when Si is replaced by Ge and finally by Sn. Third, the calculated total magnetic moments are in good agreement with the experiments in all the studied compounds except Co$_2$FeSi where a difference of 0.3 μ_B/f.u. exists. We have also performed the GGA+U calculations in order to examine the effects of the on-site Couloumb repulsion. We find that including the U changes the calculated total magnetic moment, spin polarization and AHC significantly. In most cases, unfortunately, this results in a worse agreement with the available experimental results. These interesting findings are analyzed in terms of the underlying band structures.

* jenchuan.tung@gmail.com

† gyguo@phys.ntu.edu.tw

[1] P. J. Brown, K. U. Neumann, P. J. Webster, and K. R. A. Ziebeck, J. Phys.: Condens. Matter **12**, 1827 (2000)

[2] I. Galanakis, P. H. Dederichs, and N. Papanikolaou, Phys. Rev. B **66**, 174429 (2002)

[3] J. Kübler, G. H. Fecher, and C. Felser, Phys. Rev. B **76**, 024414 (2007)

[4] H. C. Kandpal, G. H. Fecher, and C. Felser, J. Phys. D: Appl. Phys. **40**, 1507 (2007)

[5] J. C. Tung, and G. Y. Guo, New J. Phys. **15**, 033014 (2013)

[6] D. Bombor, C. G. F. Blum, O. Volkonskiy, S. Rodan, S. Wurmehl, C. Hess, and, B. Büchner, Phys. Rev. Lett. **110**, 066601 (2013)

[7] L. Makinistian, M. M. Faiz, R. P. Panguluri, B. Balke, S. Wurmehl, C. Felser, E. A. Albanesi, A. G. Petukhov, and B. Nadgorny, Phys. Rev. B **87**, 220402(R) (2013)

[8] S. Oki, K. Masaki, N. Hashimoto, S. Yamada, M. Miyata, M. Miyao, T. Kimura, and K. Hamaya, Phys. Rev. B **86**, 174412 (2012)

[9] Z. Gercsi, A. Rajanikanth, Y. K. Takahashi, K. Hono, M. Kikuchi, N. Tezuka, and K. Inomota, Appl. Phys. Lett. **89**, 082512 (2006)

[10] S. V. Karthik, A. Rajanikanth, T. M. Nakatani, Z. Gercsi, Y. K. Takahashi, T. Furubayashi, K. Inomota and K. Hono, J. Appl. Phys. **102**, 043903 (2007)

[11] K. Hamaya, N. Hashimoto, S. Oki, S. Yamada, M. Miyao, and T.Kimura, Phys. Rev. B **85**, 100404(R) (2012)

[12] S. V. Karthik, A. Rajanikanth, Y. K. Takahashi, T. Ohkubo, and K. Hono, Acta. Mater. **55**, 3867 (2007)

[13] I.-M. Imort, P. Thomas, G. Reiss, and A. Thomas, J. Appl. Phys. **111**, 07D313 (2012)

[14] Y. Wu, J. Zhang, Q. Xiong, S. Gao, X. Xu, J. Miao, Z. He, and Y. Jiang, Appl. Phys. Expr. **6**, 113003 (2013)

[15] T. Yukiko, A. Srinivasan, B. Varaprasad, A. Rajanikanth, S. Jaivardhan, H. Masamitsu, F. Takao, K. Shinya, H. Shigeyuki, M. Seiji, H. Kazuhiro, United State Patent No. 20130302649.

[16] S. Wurmehl, G. H. Fecher, H. C. Kandpal, V. Ksenofontov, C. Felser, H.-J. Lin and J. Morais, Phys. Rev. B **72**, 184434 (2005).

[17] J. P. Perdew, K. Burke, and M. Ernzerhof, Phys. Rev. Lett. **77**, 3865 (1996)

[18] A. I. Liechtenstein, V. I. Anisimov, and J. Zaanen, Phys. Rev. B **52**, 5467 (1995).

[19] E. H. Hall, Philos. Mag. **12**, 157 (1881)

[20] N. Nagaosa, J. Sinova, S. Onoda, A. H. MacDonald, and N. P. Ong, Rev. Mod. Phys. **82**, 1539 (2010)

[21] Y. Yao, L. Kleinman, A. H. MacDonald, J. Sinova, T. Jungwirth, D.-S. Wang, E. Wang, and Q. Niu, Phys. Rev. Lett. **92**, 037204 (2004)

[22] E. Roman, Y. Mokrousov, and I. Souza, Phys. Rev. Lett. **103**, 097203 (2009)

[23] H.-R. Fu and G.-Y. Guo, Phys. Rev. B **84**, 144427 (2011)

[24] J.-C. Tung, H.-R. Fuh, and G.-Y. Guo, Phys. Rev. B **86**, 024435 (2012)

[25] C. Zeng, Y. Yao, Q. Niu, and H. H. Weitering, Phys. Rev. Lett. **96**, 037204 (2006)

[26] P. He, L. Ma, Z. Shi, G. Y. Guo, J.-G. Zheng, Y. Xin, and S. M. Zhou, Phys. Rev. Lett. **109**, 066402 (2012)

[27] I. Turek, J. Kudrnovsky and V. Drchal, Phys. Rev. B **89**, 064405 (2014)

[28] J. Kübler, and C. Felser, Phys. Rev. B **85**, 012405 (2012)

[29] E. V. Vidal, G. Stryganyuk, H. Schneider, C. Felser, and G. Jakob, Appl. Phys. Lett. **99**, 132509 (2011)

[30] S. Murakami, N. Nagaosa, and S.-C. Zhang, Science **301**, 1348 (2003)

[31] L. Liu, C.-F. Pai, Y. Li, H.-W. Tseng, D. C. Ralph, and R. A. Buhrman, Science **301**, 1348 (2012)

[32] P. Grüberg, R. Schreiber, Y. Pang, M. B. Brodsky, and H. Sowers, Phys. Rev. Lett. **57**, 2442 (1986)

[33] M. N. Baibich, J. M. Broto, A. Fert, F. N. V. Dau, F. Petroff, P. Etienne, G. Creuzet, A. Friederich, and J. Chazelas, Phys. Rev. Lett. **61**, 2472 (1988)

[34] J. S. Moodera, L. R. Kinder, T. M. Wong, and R. Meservey, Phys. Rev. Lett. **74**, 3273 (1995)

[35] S. S. Parkin, C. Kaiser, A. Panchula, P. M. Rice, B. Hughes, M. Samant, and S. H. Yang, Nat. Matter. **3**, 862 (2004)

[36] J. C. Slonczewski, J. Magn. Magn. Mater. **159**, L1 (1996)

[37] E. B. Myers, D. C. Ralph, J. A. Katine, R. N. Louie, and R. A. Buhrman, Science **285**, 867 (1999)

[38] P. Blaha, K. Schwarz, G. Madsen, D. Kvasnicka, and J. Luitz *WIEN2K, An Augmented Plane Wave Local Orbitals Program for Calculating Crystal Properties* (Technische University Wien, Austria, 2002) (2012)

[39] P. B. Blöchl, O. Jepseno, O. K. and Anderson, Phys. Rev. B **49**, 16223 (1994)

[40] B. Balke, S. Wurmehl, G. H. Fecher, C. Felser, M. C. M. Alves, F. Bernardi, and J. Morais, Appl. Phys. Lett. **90**, 172501 (2007)

[41] K. H. J. Buschow, P. G. van Engen, and R. Jongebreur, J. Magn. Magn. Mater. **38**, 1 (1983)

[42] S. Wurmehl, G. H. Fecher, H. C. Kandpal, V. Ksenofontov, C. Felser, H. J. Lin, and J. Morais, Phys. Rev B **72**, 184434 (2005)

[43] K. R. A. Ziebeck, and K.-U. Neumann *Alloys and Compounds of d-Elements with Main Group Elements, Part 2 (Landolt-Börnstein, Group III Condensed Matter* vol 32C) (Heidelberg: Springer) (Heusler Alloys) pp 64-314 (2001)

[44] K. R. Kumar, K. K. Bharathi, J. A. Chelvane, S. Venkatesh, G. Markandeyulu, and N. Harishkumar, IEEE Trans. Magn. **45**, 3997 (2009)

[45] T. M. Nakatani, A. Rajanikanth, Z. Gercsi, Y. K. Takahashi, K. Inomata, and K. Hono, J. Appl. Phys. **102**, 033916 (2007)

[46] M. A. Tanaka, Y. Ishikawa, Y. Wada, S. Hori, A. Murata, S. Horii, Y. Yamanishi, K. Mibu, K. Kondou, T. Ono, and S. Kasai, J. Appl. Phys. **111**, 053902 (2012)

[47] G. Y. Guo, and H. Ebert, Phys. Rev B **51**, 12633 (1995)

[48] G. Y. Guo, Y. Yao, and Q. Niu, Phys. Rev. Lett. **94**, 226601 (2005)

[49] G. Y. Guo, S. Murakami, T.-W. Chen, and N. Nagaosa, Phys. Rev. Lett. **100**, 096401 (2008)

[50] G. Y. Guo, Q. Niu and N. Nagaosa, Phys. Rev B **89**, 214406 (2014)

[51] R. J. Soulen Jr., J. M. Byers, M. S. Osofsky, B. Nadgorny, T. Ambrose, S. F. Cheng, P. R. Broussard, C. T. Tanaka, J. Nowak, J. S. Moodera, A. Barry, and J. M. D. Coey, Science **282**, 85 (1998)

[52] J. M. De Teresa, A. Barthélémy, A. Fert, J. P. Contour, F. Montaigne, and P. Seneor, Science **286**, 507 (1999)

[53] P. A. Dowben, N. Wu, and C. Binek, J. Phys.:Condens. Matter **23**, 171001 (2011)

[54] X. Kozina, J. Karel, S. Ouardi, S. Chadov, G. H. Fecher, and C. Felser, G. Stryganyuk, B. Balke, T. Ishikawa, T. Uemura, M. Yamamoto, and E. Ikenaga, Phys. Rev. B **89**, 125116 (2014)

[55] G. K. H. Madsen, and D. J. Singh, Comput. Phys. Commum. **175**, 67 (2006)

[56] The experimental b values[6,13,14,57] listed in Table II were obtained by fitting the expression $\rho_A = a\rho_{xx} + b\rho_{xx}^2$ to the measured anomalous Hall resistivity ρ_A. The coefficient b is the scattering-independent term containing both the intrinsic and extrinsic side-jump contributions while the coefficient a is the extrinsic skew-scattering term[20].

[57] E. V. Vidal, H. Schneider and G. Jakob, Phys. Rev. B **83**, 174410 (2011)

[58] G. H. Fecher and C. Felser, J. Phys. D: Appl. Phys. **40**, 1582 (2007)

[59] Y.-F. Hsu, T.-W. Chiang, G. Y. Guo, S. F. Lee and J.-J. Liang, J. Phys. Soc. Jpn **81**, 084701 (2012)